UDC 546.26-162

S. E. Boulfelfel, Q. Zhu (New York, US)
A. R. Oganov (New York, US, Moscow, Russia)

Novel sp^3 forms of carbon predicted by evolutionary metadynamics and analysis of their synthesizability using transition path sampling

Experiments on cold compression of graphite have indicated the existence of a new superhard and transparent allotrope of carbon. Numerous metastable candidate structures featuring different topologies have been proposed for "superhard graphite", showing a good agreement with experimental X-ray data. In order to determine the nature of this new allotrope, we use evolutionary metadynamics to systematically search for low-enthalpy sp^3 carbon structures easily accessible from graphite and we employ molecular-dynamics transition path sampling to investigate the corresponding kinetic pathways starting from graphite at 15–20 GPa. Real transformation kinetics are computed and physically meaningful transition mechanisms are produced at the atomistic level of detail in order to demonstrate how nucleation mechanism and transformation kinetics lead to M-carbon as final product of cold compression of graphite. This establishes M-carbon as an experimentally synthesized carbon allotrope.

Keywords: *high pressure, carbon, polymorphism, superhard material, molecular dynamics, metadynamics.*

INTRODUCTION

One of the major challenges of the 21st century has been the quest for novel materials with superior physical properties, which has led to a high demand on computational materials design. Theoretical methodologies for structure prediction [1] have recently seen a remarkable progress demonstrated by important discoveries [2, 3] of new forms of solid state materials with interesting physical properties. One of the physical properties relevant for both fundamental science and advanced technology is hardness [4]. Despite numerous efforts [1, 5–7] to discover new superhard materials, diamond is still widely regarded as the hardest of all known materials [8]. Experimentally, the thermodynamically stable high pressure structure of cubic diamond is formed at high pressures and temperatures (> 5 GPa and 1200–2800 K). At room temperature, however, a new transparent and superhard phase is obtained at pressures above 15 GPa [9–12], which is different from cubic diamond and its hexagonal polytype lonsdaleite. The lack of obvious structural model for this new phase has stimulated theoretical efforts [13–18]. Several metastable candidate structures have been proposed, e.g., M-carbon [13, 19], bct-C_4 [14, 15, 20], W-carbon [16], and oC16-II [17, 18]. The experimental observations of X-ray diffraction, superhardness and transparency of cold compressed graphite can be explained by these structures and their band gaps [13–18, 20]. In order to resolve this problem, we use the recently proposed evolutionary metadynamics method to efficiently explore different local minima on the potential

energy surface of elemental carbon to construct a list of all candidate structures. Then we employ transition path sampling simulations to tackle the kinetics and structural reconstruction mechanism of graphite upon cold compression and to elucidate the nature of the kinetically likeliest allotrope to form.

METHODOLOGY

Evolutionary metadynamics

The main idea of metadynamics consists in the introduction of a history-dependent potential term, which gradually fills the minima in the free energy surface and discourages the system to go back to its previously visited states until the system could cross the energy barriers and undergo phase transitions [21]. This method is usually applied in combination with molecular dynamics simulations [22]. Because it relies on molecular dynamics (MD) for equilibration, the simulation is often trapped in metastable states and can amorphize instead of transforming into a (meta)stable crystal structure. To overcome this, we recently introduced a metadynamics-like hybrid method based on efficient global optimization of moves rather than local MD sampling [19, 23].

In this method [24], the simulation is started from a known initial structure at a given external pressure P. The cell vectors matrix h_{ij} (6-dimensional vector h) is used as a collective variable to monitor structural changes in the system [22]. Considering a given system with volume V under external pressure P, the derivative of the free energy G with respect to h can be expressed as:

$$-\frac{\partial G}{\partial h_{ij}} = V[h^{-1}(P-p)]_{ji} . \qquad (1)$$

At each metastep, many structures are generated and relaxed at fixed h, and the lowest energy structure is selected and its internal tensor p is computed. Unlike in the previously proposed scheme [22], many structures are produced at each metastep in this hybrid method [24], instead of only one. Using stepping parameter δh, the cell shaped is updated as the following:

$$h_{im}(t+1) = h_{im}(t) + \frac{\delta h}{|f|V^{1/3}} S_{ijkl} f_{kl} h_{jm}(t) , \qquad (2)$$

here S is the elastic compliance tensor. It corresponds to an elastically isotropic medium with the Poisson ratio of 0.26, which represents the border value between brittle and ductile materials [25], and is a good average value to describe both metals and insulators. The driving force $f = -\frac{\partial G}{\partial h}$ in Eq. (2) comes from a history-dependent Gibbs potential G^t. For each point already visited $h(t')$, a Gaussian is added to $G(h)$ in order to discourage the system from visiting it again,

$$G(t) = G^h + \sum W e^{-\frac{|h-h(t')|^2}{2\delta h^2}} , \qquad (3)$$

here W is the Gaussian height. In the next step, the vibrational modes for the selected structure are computed according to the dynamical matrix constructed from bond hardness coefficients,

$$D_{\alpha\beta}(a,b) = \sum_m \left(\frac{\partial^2}{\partial\alpha_a^0 \partial\beta_b^m} \frac{1}{2} \sum_{i,j,l,n} H_{i,j}^{l,n} (r_{i,j}^{l,n} - r_{0i,j}^{l,n})^2 \right). \quad (4)$$

Here atoms in the unit cell are indexed by a, b, i, j. Their coordinates (x, y, z) are denoted by α and β. Unit cells are indexed by l, m, n. The distance between atom i in the unit cell l and atom j in the unit cell n is denoted by $r_{i,j}^{l,n}$, while bond distance is associated with $r_{0i,j}^{l,n}$. The bond hardness coefficient, $H_{i,j}^{l,n}$, is computed from bond distances, covalent radii and electronegativity of the atoms [23].

The computed vibrational modes are used to produce a new generation (typically 20–40 soft-mutated structures each from a particular normal mode). The softmutation [23, 24] is performed by moving the atoms along the eigenvector of the softest calculated mode. Using different non-degenerate modes and displacements, each structure can be softmutated many times. The magnitude of the displacement ($d_{\max}$) along the mode eigenvector is an input parameter. Using relatively small $d_{\max}$ and displacements represented by a random linear mixture of all mode eigenvectors, this method becomes similar to MD-metadynamics in its ability to cross energy barriers and equilibrate the system. Using large $d_{\max}$ along single softest-mode eigenvectors, the softmutation operator [23] is capable of efficiently finding the global energy minimum.

The new generation of softmutated structures is produced and relaxed in the new cell. The process is repeated for a number of generations, and a series of structural transitions are observed. The simulation is stopped when the maximum number of generations is reached.

Zhu et al. [26] used evolutionary metadynamics to systematically find low-enthalpy superhard allotropes accessible from graphite. Evolutionary metadynamics simulations were done using the USPEX code [19]. In this work, structural relaxations were performed using density functional theory (DFT) within the generalized gradient approximation (GGA) [27] in the framework of the all-electron projector augmented wave (PAW) method [28], as implemented in the VASP [29, 30] code. A plane wave kinetic energy cutoff of 550 eV is used for the plane–wave basis set. Excellent convergence of the energy differences, stress tensors, and structural parameters was ensured by using Brillouin zone sampling resolution of $2\pi\times0.08$ Å^{-1}.

Transition path sampling (TPS)

TPS is a generalization of Monte Carlo procedures in the space of dynamical trajectories connecting two states separated by a high barrier in a rough energy landscape [31–33]. The simulation scheme is iterative and develops from an initial trajectory. The first step of transition path sampling consists of equilibration of an initial pathway, then, gradually converging the trajectory regime to more probable regions. To ensure convergence of the transition regime, the relevance of a transition pathway is biased by path probability. It is worth mentioning that no a priori knowledge of the mechanistic details of the real transition regime is needed to start the sampling of pathways. Consequently, the first trajectory does not need to be a probable one.

The first step is the derivation of an initial trajectory connecting the limiting phases. A configuration from latter trajectory is selected and the atomic momenta are slightly modified. While keeping both momentum and angular momentum

conserved, the modifications δp are applied to randomly chosen pairs of atoms (i, j) as follows:

$$\vec{p}_i^{new} = \vec{p}_i^{old} + \delta p(\vec{r}_j - \vec{r}_i)/\left|(\vec{r}_j - \vec{r}_i)\right|; \quad (5)$$

$$\vec{p}_j^{new} = \vec{p}_j^{old} - \delta p(\vec{r}_j - \vec{r}_i)/\left|(\vec{r}_j - \vec{r}_i)\right|. \quad (6)$$

In order to keep the total kinetic energy conserved, the modified atomic momenta are rescaled by the factor:

$$\sqrt{E_{kin}^{old}/(\sum_i \left|\vec{p}_i^{new}\right|^2/2m_i)}. \quad (7)$$

The modified configuration is propagated in both directions of time ($-t$, $+t$) and a new trajectory is generated. If the latter is successful (the transition is observed), it is used as an initial trajectory in a new iteration and the procedure is iterated to collect a set of pathways. The successful ones are selected and analyzed.

In this work, Born-Oppenheimer molecular dynamics simulations were performed in the *NpT* ensemble [34] at temperature T = 300 K and pressures ranging from 15 to 20 GPa. The time propagation of the system was performed using the velocity Verlet algorithm [34], with an integration timestep of 0.2 fs, in order to maintain a good time–reversibility for the collected trajectories. The simulation box contained 256 carbon atoms. To allow for anisotropic shape changes of the simulation box, the Martyna-Tobias-Klein algorithm [35] for ensuring constant pressure and temperature was used. Interatomic forces were computed within the framework of density-functional tight binding approach [36, 37] as implemented in the CP2K code [38]. For each transition path sampling run, the number of trial shootings was at least 500, with an acceptance ratio between 40–60 %. More than 200 successful pathways have been collected for each run, of which ~ 70 are independent and uncorrelated. The average coordination number (CN) within the first coordination sphere is used as an order parameter to distinguish graphite (CN = 3) from high pressure modifications made of four-coordinate atoms (CN = 4). To distinguish between different four-coordinate structures (bct-C_4, M-carbon, and W-carbon), however, coordination spheres of second and third nearest neighbors are used. This helps to narrow down the path ensemble and focus the sampling on transition from graphite to one of the candidate structures for "superhard graphite". Apart from a quick detection of graphite and different candidate structures (bct-C_4, M-carbon, and W-carbon), this order parameter is capable of accommodating not only the three possible metastable phases but allows for starting transition pathways sampling from unlikely trajectories, like graphite to cubic or hexagonal diamond, and converge to the likeliest trajectory that starts with graphite and leads to the kinetically most probable end product of its room-temperature compression.

RESULTS AND DISCUSSION

Let us first discuss the results of the systematic search and identification of possible structures of "superhard graphite" using evolutionary metadynamics [26]. Simulations were started from two different graphite polytypes, 2H and 3R.

Starting from graphite-2H model containing 32 atoms, a simulation was performed at 20 GPa (d_{max}= 2.5 Å, W = 4000 kbar·Å^3, and δh = 0.6 Å). At each metastep, the best structure from the previous generation was softmutated by

25 times. While the ground state structure was identified as cubic diamond, many metastable structures were found. As shown in Fig. 1, *a*, a series of structures is visited during the simulation. After 15 generations, layers buckling is observed and graphite planar structure is transformed into 3D-networks of sp^3-hybridized carbon

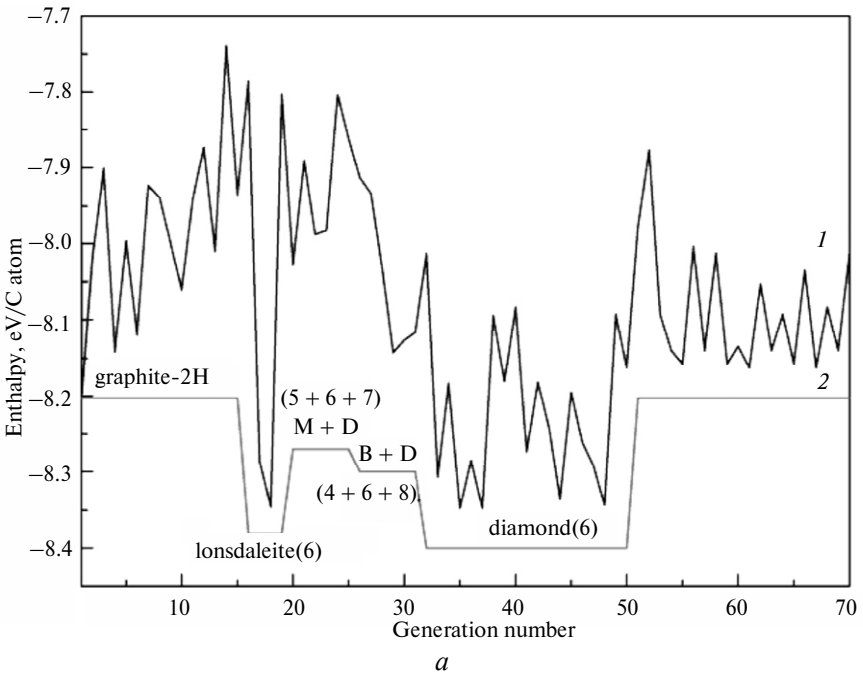

Fig. 1. Enthalpy evolution during the compression of graphite-2H at 20 GPa (*a*); enthalpy evolution during the compression of graphite-3R at 20 GPa ((*1*) enthalpies for the best structures with constant cell matrix, (*2*) enthalpies for best structures after full relaxation) (*b*). The corresponding ring topologies are shown in parentheses. B + D and M + D refer to bct-C_4 + diamond and M-carbon + diamond, respectively.

atoms. Lonsdaleite is identified as the best structure in the 16th generation, and in the same generation we observed a candidate structure with 4 + 8 membered rings, bct-C_4 (Fig. 2, *c*). Structural patterns featuring 5 + 7 membered rings are observed in the subsequent generations and corresponds to M- and W-carbon (Figs. 2, *d*, *e*). These are followed by another mixed system of *M*-carbon interfaced with diamond (referred to as $M + D$, featuring 5 + 6 + 7 membered rings). Another structure, containing blocks of bct-C_4 interfaced with diamond, is obtained in the following generations (referred to as $B + D$ in Fig. 2, *f*) buckling. Described as a stacking of layers of 4 + 8 and 6-membered rings, it is equivalent to o*C*16 structure (also called Z-carbon), another recently proposed candidate structure for "superhard graphite" [18]. The last episode of the simulation is characterized by a dominance of the diamond structure for almost 20 generations, before the system reverted to graphite.

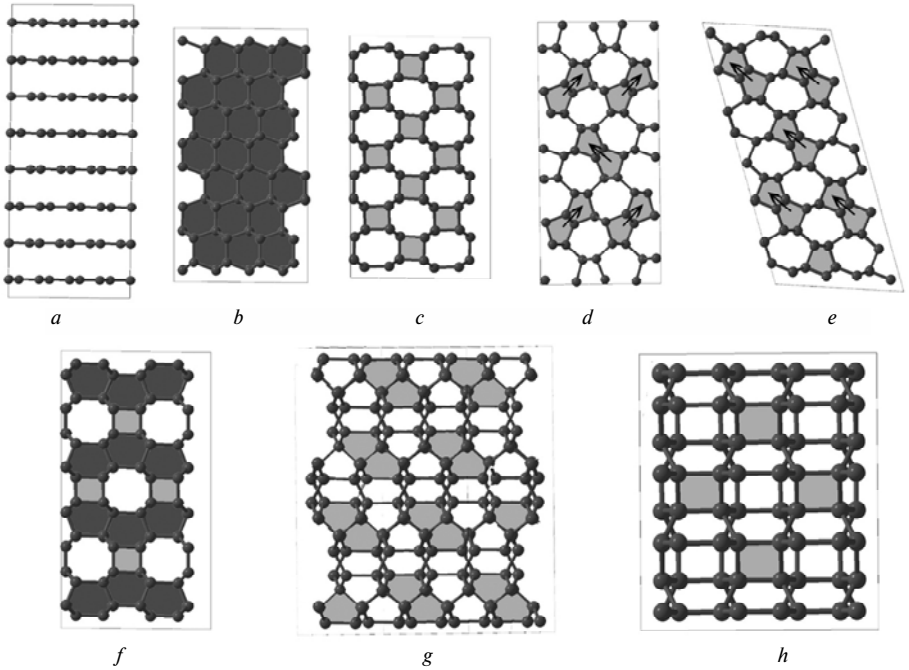

Fig. 2. Structures obtained using evolutionary metadynamics: graphite-2H (*a*), polytype of diamond with 6 topology (*b*), bct-C_4 with 4 + 8 topology (*c*), M-carbon with 5 + 7 topology (*d*), W-carbon with 5 + 7 topology (*e*), Z-carbon with 4 + 6 + 8 topology (*f*), new allotrope X-carbon with 5 + 7 topology (*g*). Its space group is *C*2/*c*, a = 5.559 Å, c = 4.752 Å, b = 7.960 Å, β = 114.65°, C1(0.250, 0.083, 0.949), C2(0.489, 0.809, 0.982), C3(0.000, 0.200, 0.250), C4(0.247, 0.913, 0.801), C5(0.000, 0.816, 0.250); new allotrope Y-carbon with 4 + 8 topology (*h*). Its space group is *Cmca*, a = 4.364 Å, c = 4.374 Å, b = 5.057 Å, C(0.681, 0.635, 0.410).

Similarly starting from graphite-3R at 20 GPa, diamond is again identified as the ground state structure after visiting a series of low-energy metastable structures as shown in Fig. 1, *b*.

The power of evolutionary metadynamics method is in its efficiency in harvesting, in addition to the ground state, many low-energy metastable structures in a single simulation (see Fig. 2). Clearly, all of the previously reported candidate structures for "superhard graphite" (M-, W-, bct-C_4, and Z-carbon) could be easily found in using 1-2 evolutionary metadynamics simulations. Most strikingly, two new topologically different structures are discovered during the simulations, which

we call X- and Y-carbon. The first one (Fig. 2, *g*) has 5 + 7 topology with a monoclinic symmetry (space group *C*2/*c*) and contains 32 carbon atoms in the conventional cell. The second structure (Fig. 2, *h*) has 4 + 8 topology with an orthorhombic symmetry (space group *Cmca*) and contains 16 atoms in the conventional cell. Note that there are also many hybrid structures made of alternating layers of M-carbon, bct-C_4 diamond and lonsdaleite (for the detailed information, please refer to Ref. [26]).

In general, low-enthalpy metastable structures are extremely reachable. In the case of cold-compressed graphite, many candidate structures for "superhard graphite", including X- and Y-carbon, show a good agreement with experimental XRD data as shown in Fig. 3. The nature of the product depends on the structure of the starting material, the energy landscape and kinetic barriers separating the transforming phases. Transition path sampling is a very helpful simulation strategy to tackle a situation characterized by the possibility of many theoretically viable candidate structures. The method allows starting from a regime of very low probability or even a model constructed from a mapping between the limiting phases of the transition of interest. Monte Carlo sampling of the space of trajectories ensures the convergence toward the real transformation path and unveils the nature of "superhard graphite".

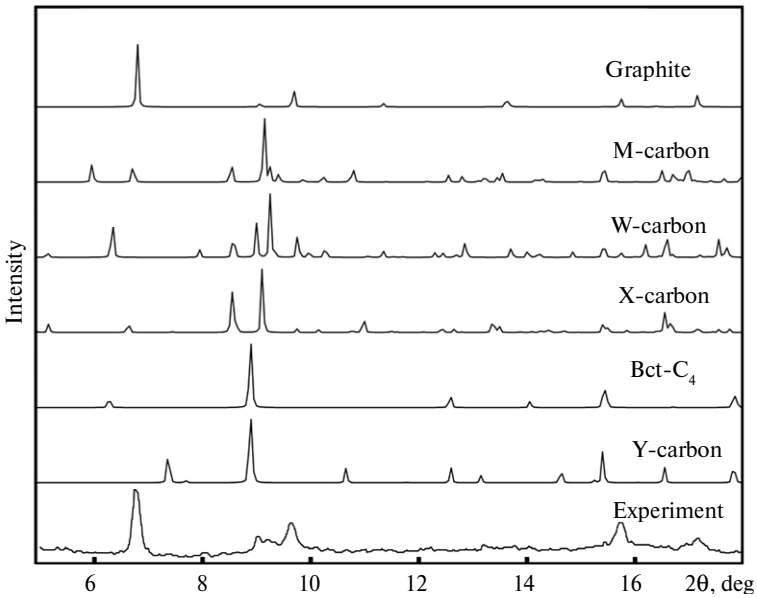

Fig. 3. Simulated X-ray diffraction patterns (from Ref. [26]) of proposed models and graphite compared with experiment [12]; the pressure being 18.4 GPa.

The second part of this work is concerned with finding the real transition route of cold compressed graphite and the identification of the "superhard graphite" structure using TPS simulations [39]. We started TPS runs from trajectories connecting graphite-2H to diamond. Since diamond was ruled out by experiments [41], the sampling of graphite–diamond route will not only optimize the transition regime, but will help converging to a kinetically more probable structure for the product of cold compression of graphite.

The set of pathways collected in the course of TPS iterations shows a quick shift in the transition regime. After only 15–20 iterations, the end-point of the initial graphite–diamond pathway is replaced by a polytype of the diamond

structure as shown in Fig. 4, *e*. The sliding of graphene layers in opposite directions is responsible for the appearance of this polytype, intermediate between diamond and lonsdaleite. After only 30–40 iterations, new structural patterns of 5 + 7 rings is observed in the form of an inset within 6-membered ring topology as highlighted in Fig. 5, *e* by a dotted circle. Despite the small size of the inset, not allowing for clear identification of its symmetry, the 5 + 7 pattern is a signature of some metastable structures observed during evolutionary metadynamics simulations, e.g., M- and W-carbon. Upon further sampling of the trajectory ensemble, 6-membered rings are replaced by 5 + 7 ones, as the inset grows larger and diamond converts into a distinct configuration with monoclinic symmetry. This structure is identical to the metastable allotrope M-carbon, first predicted in [19] and later proposed to correspond to "superhard graphite" [13].

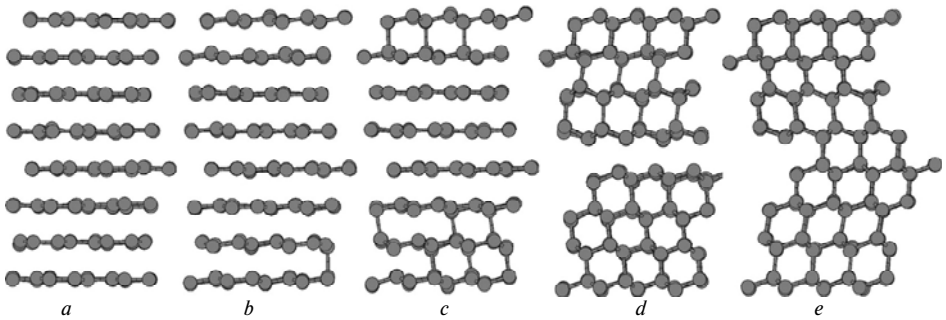

Fig. 4. Snapshots from a dynamical trajectory collected from transition path sampling connecting graphite (*a*) to a diamond polytype (*e*). The buckling of graphite layers is initiated by the formation of C–C bonds along the $[001]_{graphite}$ (*b*). Domains of cubic diamond are formed with different orientation (*c*)–(*d*). The interface between the latter domains defines a region of hexagonal diamond (*e*).

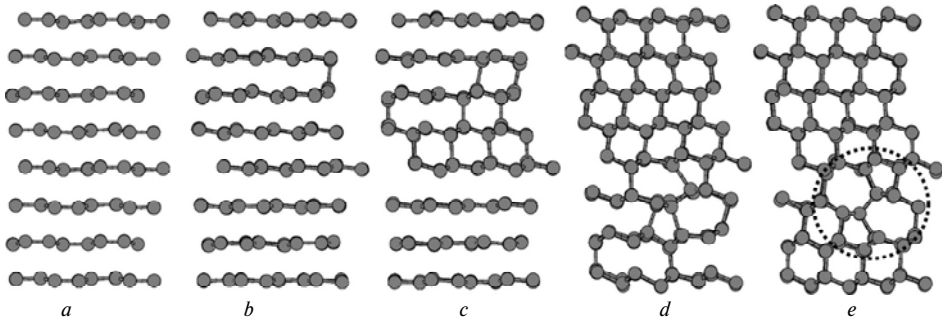

Fig. 5. Snapshots from a representative trajectory illustrating the evolution of graphite (*a*) to cubic diamond transition regime (*e*). The mobility of graphene layers during the reconstruction creates an inset of 5- and 7-membered rings (dotted circle) within a 6-membered rings network (*e*).

As shown in Fig. 6, the onset of the transformation is marked by the formation of interlayer C–C bonds along the $[001]_{graphite}$ in a zigzag fashion (see Fig. 6, *b*). The π-interactions in graphene layers are perturbed by the formation of the zigzag chain. Consequently, layer corrugation is facilitated and 5-and 7-membered rings are formed during layers buckling, as illustrated in Figs. 6, *c*–*e*. Although, M-carbon is identified as the most probable structure to be formed upon cold compression of graphite, the transition regime visited other 5 + 7 topologies before locking into the stable graphite to M-carbon transformation route.

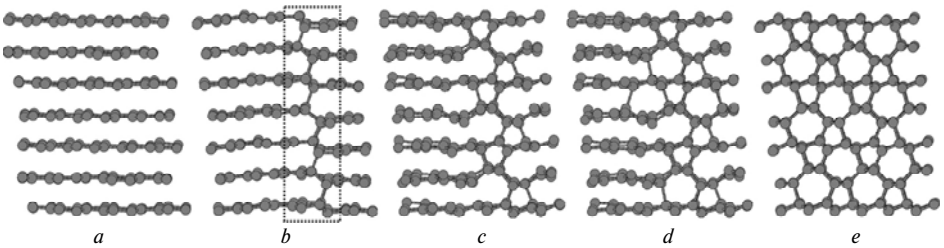

Fig. 6. Snapshots of a representative trajectory of the stable regime corresponding to the cold compression of graphite. A single event of bond formation between graphene layers triggers (*a*), a series of bond formation along [001] graphite in a zigzag fashion (dotted rectangle) (*b*). This chain facilitates the formation of 5-membered rings causing the corrugation of graphitic layers (*c*) and inducing the formation of 7-membered rings (*d*)–(*e*).

Up to 20% of the successful trajectories collected during the sampling included graphite to W-carbon pathway shown in Fig. 7. Despite similarities in nucleation events between graphite to M-carbon and graphite to W-carbon in terms of the formation of C–C bonds along $[001]_{graphite}$, subsequent growth of W-carbon slightly differs from that of M-carbon. Unlike the transition mechanism of graphite to M-carbon, the zigzag chain is propagated in a segmented fashion (see Fig. 7, *b*). Clearly, the key step that determines the nature of the cold compression product is the evolution of a single nucleation event, formation of an interlayer C–C bond, either as infinite zigzag (see Fig. 6, *b*) or segmented chain (see Fig. 7, *b*). Furthermore, the breaking of the chain implies different progress of phase growth and results in a higher transition barrier as shown in Fig. 8.

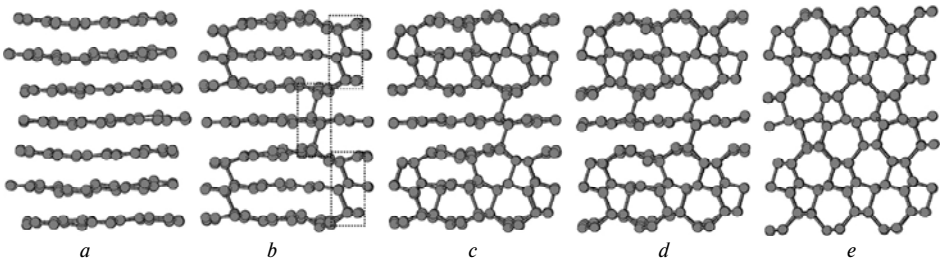

Fig. 7. Snapshots taken from a representative graphite to W-carbon transformation pathway. Graphene layers buckling is initiated by formation C–C contacts along $[001]_{graphite}$ in the form of finite size zigzag chains (*b*). Each zigzag chain facilitates the corrugation of graphitic layers inducing the formation of 5-and 7-membered rings (*c*)–(*d*) transforming graphite into W-carbon (*e*).

It is worth mentioning that the layered structure of graphite theoretically enables many different ways of layers buckling. Each of them may lead to a different final topology and distinct structure. From TPS simulations, we conclude that the survival of a transition regime leading to one metastable structure or another is closely connected to the way of nucleating the high-pressure modification and the corresponding activation barrier. One of the advantages of using TPS is its efficiency to converge to the relevant path ensemble, which corresponds to the real transition pathway regime [31–33, 42–46] and bypasses less-favored regions of the energy landscape corresponding to other mechanisms, e.g., graphite to bct-C_4 pathway. To illustrate this feature of TPS, we performed separate simulation runs to evaluate the energy barrier of graphite to bct-C_4 and to W-carbon transition routes in comparison with the M-carbon pathway. Figure 8 indicates that graphite

to cubic diamond transformation has a barrier of 200 meV/atm, which completely rules out the graphite to bct-C_4 route, which scores as the highest with 221 meV/atom. In spite of structural and mechanistic similarities between transformation routes to W-carbon and M-carbon, the latter is favored with a barrier equal to 176 meV/atom, lower than 194 meV/atom for the former transition [39].

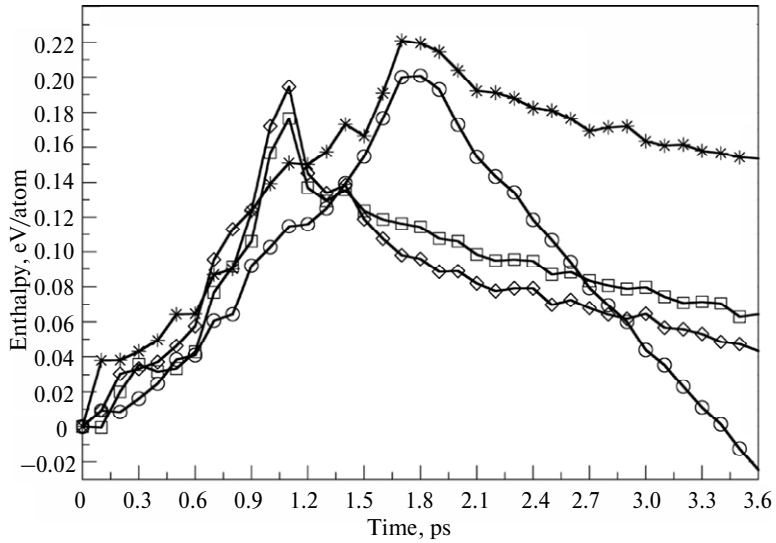

Fig. 8. Enthalpy variation of different simulated transformations of graphite under pressure (15 GPa) and ambient temperature (from Ref. [39]). The graphite to M-carbon transformation route (square line) indicates a lower energy barrier than the transition to W-carbon (diamond line). The possibility of the transformation of graphite into the bct-C_4 structure (star line) on cold compression is ruled out because of higher barrier than the graphite to cubic diamond transition (circle line).

Our findings have been subsequently confirmed and supported by a very recent investigation [40] that provided direct experimental evidence from high-quality XRD data and Raman spectroscopy. In conclusion, the nature of "superhard graphite" is elucidated using evolutionary metadynamics and transition path sampling. Combining both methods helps to systematically predict a series of metastable candidate structures and probe their synthesizability under experimental conditions of pressure and temperature. The complexity of the quest for this new superhard allotrope obtained upon compression at room temperature is clarified by the determination of intrinsic differences, at the atomistic level, between transition pathways leading to different metastable candidate structures. The product of this first-order transition is unequivocally identified as a metastable monoclinic structure, M-carbon. Although a competitor, W-carbon is kinetically less favored. Differences in transformation kinetics can be traced back to different patterns of phase nucleation and subsequent growth [39].

ACKNOWLEDGMENTS

Calculations were performed on the supercomputer of the Center for Functional Nanomaterials, Brookhaven National Laboratory, which is supported by the U.S. Department of Energy, Office of Basic Energy Sciences, under Contract No. DE-AC02-98CH10086, at the Joint Supercomputer Center of the Russian Academy of Sciences, and on the Skif supercomputer (Moscow State University). This work

used the Extreme Science and Engineering Discovery Environment (XSEDE), which is supported by National Science Foundation grant number OCI-1053575 (Project allocation TG-DMR110058). This work is funded by DARPA (No. N66001-10-1-4037), National Science Foundation (No. EAR-1114313), and Natural Science Foundation of China (No. 11174152). Evolutionary metadynamics has been implemented into the USPEX code, which is available at http://han.ess.sunysb.edu/~USPEX.

Експерименти по холодному стисненню графіту показали наявність нової надтвердої і прозорою аллотропной форми вуглецю. Численні метастабільні структури з різною топологією були запропоновані для "надтвердого графіту" і показували добру відповідність експериментальним даним рентгенографії. Для однозначного визначення природи цієї нової аллотропной форми нами використано еволюційну метадінаміку, метод, що дозволяє систематичний пошук низькоентальпійних sp^3-вуглецевих структур, що кінетично легко одержують з графіту, а також застосований молекулярно-динамічний вибір способів дослідження відповідної кінетики перетворення графіту при тисках 15–20 ГПа. Розрахована реальна кінетика перетворення графіту і отримані на атомистическому рівні реалістичні механізми перетворення, що демонструють, як механізм нуклеації та кінетика перетворення приводять до М-вуглецю – кінцевого продукту холодного стиснення графіту. Ці дослідження дозволяють вважати М-вуглець експериментально синтезованої алотропной формою вуглецю.

***Ключові слова**: високий тиск, вуглець, поліморфізм, надтверді матеріали, молекулярна динаміка, метадінаміка.*

Эксперименты по холодному сжатию графита показали наличие новой сверхтвердой и прозрачной аллотропной формы углерода. Многочисленные метастабильные структуры с различной топологией были предложены для "сверхтвердого графита" и показывали хорошее согласие с экспериментальными данными рентгенографии. Для однозначного определения природы этой новой аллотропной формы нами использована эволюционная метадинамика, метод, позволяющий систематический поиск низкоэнтальпийных sp^3-углеродных структур, кинетически легко получаемых из графита, а также применен молекулярно-динамический выбор способов исследования соответствующей кинетики превращения графита при давлениях 15–20 ГПа. Рассчитана реальная кинетика преобразования графита и получены на атомистическом уровне реалистичные механизмы превращения, которые демонстрируют, как механизм нуклеации и кинетика превращения приводят к М-углероду – конечному продукту холодного сжатия графита. Эти исследования позволяют считать М-углерод экспериментально синтезированной аллотропной формой углерода.

***Ключевые слова**: высокое давление, углерод, полиморфизм, сверхтвердые материалы, молекулярная динамика, метадинамика.*

1. *Modern* Methods of Crystal Structure Prediction / Ed. A. R. Oganov. – Weinheim, Germany: Wiley-VCH, 2010. – 274 p.
2. *Oganov A. R., Chen J., Gatti C. et al.* Ionic high-pressure form of elemental boron // Nature. – 2009. – **457**. – P. 863–867.
3. *Ma Y., Eremets M. I., Oganov A. R. et al.* Transparent dense sodium // Ibid. – 2009. – **458**. – P. 182–185.
4. *Oganov A. R., Lyakhov A. O.* Towards the theory of hardness of materials // J. Superhard Mater. – 2010. – **32**, N 3. – P. 143–147.
5. *Gao F., He J., Wu E. et al.* Hardness of covalent crystals // Phys. Rev. Let. – 2003. – **91**, art. 015502.
6. *Simunek A., Vackar J.* Hardness of covalent and ionic crystals: first-principle calculations // Ibid. – 200. – **96**, art. 085501.
7. *Li K., Wang X., Zhang F., Xue D.* Electronegativity identification of novel superhard materials // Ibid. – 2008. – **100**, art. 235504.
8. *Pan Z., Sun H., Zhang Y., Chen C.* Harder than diamond: superior indentation strength of wurtzite BN and lonsdaleite // Ibid. – 2009. – **102**, art. 055503.

9. *Aust R. B., Drickamer H. G.* Carbon: a new crystalline phase // Science. – 1963. – **140**. – P. 817–819.
10. *Bundy F. P., Kasper J. S.* Hexagonal diamond – a new form of carbon // J. Chem. Phys. – 1967. – **46**. – P. 3437–3446.
11. *Utsumi W., Yagi T.* Light-transparent phase formed by room-temperature compression of graphite // Science. – 1991. – **252**. – P. 1542–1544.
12. *Mao W. L., Mao H. K., Eng P. J. et al.* Bonding changes in compressed superhard graphite // Ibid. – 2003. – **302**. – P. 425–427.
13. *Li Q., Ma Y., Oganov A. R., Wang H. et al.* Superhard monoclinic polymorph of carbon // Phys. Rev. Lett. – 2009. – **102**, art. 175506.
14. *Umemoto K., Wentzcovitch R. M., Saito S., Miyake T.* Body-centered tetragonal C_4: a viable sp^3 carbon allotrope // Ibid. – 2010. – **104**, art. 125504.
15. *Zhou X. F., Qian G. R., Dong X. et al.* Ab initio study of the formation of transparent carbon under pressure // Phys. Rev. B. – 2010. – **82**, art. 134126.
16. *Wang J.-T., Chen C., Kawazoe Y.* Low-temperature phase transformation from graphite to sp^3 orthorhombic carbon // Phys. Rev. Lett. – 2011. – **106**, art. 075501.
17. *Zhao Z., Xu B., Zhou X. F. et al.* Novel superhard carbon: C-centered orthorhombic C_8 // Ibid. – 2011. – **107**, art. 215502.
18. *Selli D., Baburin I., Martinek R. Leoni S.* Superhard sp^3 carbon allotropes with odd and even ring topologies // Phys. Rev. B. – 2011. – **84**, art. 161411(R).
19. *Oganov A. R., Glass C. W.* Crystal structure prediction using *ab initio* evolutionary techniques: principles and applications // J. Chem. Phys. – 2006. – **124**, art. 244704.
20. *Baughman R. H., Liu A. Y., Cui C., Schields P. J. A* Carbon phase that graphitizes at room temperature // Synth. Met. – 1997. – **86**. – P. 2371–2374.
21. *Laion A., Parrinello M.* Escaping free-energy minima // Proc. Natl. Acad. Sci. of the USA. – 2002. – **99**. – P. 12562–12566.
22. *Martinek R., Laion A., Parrinello M.* Predicting crystal structures: the Parrinello-Rahman method revisited // Phys. Rev. Lett. – 2003. – **90**, art. 07550.
23. *Lyakhov A. L., Oganov A. R., Valle M.* How to predict very large and complex crystal structures // Comp. Phys. Comm. – 2010. – **181**. – P. 1623–1632.
24. *Zhu Q., Oganov A. R., Lyakhov A. L.* Evolutionary metadynamics: a novel method to predict crystal structures // CrystEngComm. – 2010. – **14**. – P. 3596–3601.
25. *Pugh S. F.* Relations between elastic moduli and plastic properties of polycrystalline pure metals // Philos. Mag. – 1954. – **45**. – P. 823–843.
26. *Zhu Q., Zeng Q., Oganov A. R.* Systematic search for low-enthalpy sp^3 carbon allotropes using evolutionary metadynamics // Phys. Rev. B. – 2012. – **85**, art. 01407.
27. *Perdew J. P., Burke K., Ernzerhof M.* Generalized gradient approximation made simple // Phys. Rev. Lett. – 1996. – **77**. – P. 3865–3868.
28. *Blöchl P. E.* Projector Augmented-wave method // Phys. Rev. B. – 1994. – **50**. – P. 17953–17979.
29. *Kresse G., Joubert D.* From ultrasoft pseudopotentials to the projector augmented-wave method // Ibid. – 1994. – **59**. – P. 1758–1775.
30. *Kresse G., Furthmüller J.* Efficient iterative schemes for *ab initio* total-energy calculations using a plane-wave basis set // Ibid. – 1996. – **54**. – P. 11169–11186.
31. *Bolhuis P. G., Dellago C., Chandler D.* Sampling ensembles of deterministic transition pathways // Faraday Discuss. – 1998. – **110**. – P. 421–436.
32. *Dellago C., Bolhuis P. G., Csajka F. S., Chandler D.* Transition path sampling and the calculation of rate constants // J. Chem. Phys. – 1998. – **108**. – P. 1964–1978.
33. *Bolhuis P. G., Chandler D., Dellago C., Geissler P. L.* Transition path sampling: throwing ropes over rough mountain passes, in the dark // Annu. Rev. Phys. Chem. – 2002. – **3**. – P. 291–318.
34. *Frenkel D., Smit B.* Understanding molecular simulations from algorithms to applications. – 2nd Ed. – San Diego: Academic, 2002. – 638 p.
35. *Martyna G. J., Tobias D. J., Klein M. L.* Constant pressure molecular dynamics algorithms // J. Chem. Phys. – 1994. – **101**. – P. 4177–4190.
36. *Seifert G., Porezag D., Frauenheim Th.* Calculations of molecules, clusters, and solids with a simplified LCAO-DFT-LDA scheme // Int. J. Quant. Chem. – 1996. – **58**. – P. 185–192.
37. *Zhechkov L., Heine T., Patchkovskii S. et al.* An efficient a posteriori treatment for dispersion interaction in density-functional-based tight binding // J. Chem. Theo. Comp. – 2005. – **1**. – P. 841–847.

38. *http://cp2k.berlios.de (2011).*
39. *Boulfelfel S. E., Oganov A. R., Leoni S.* Understanding the nature of “superhard graphite”. – Sci. Rep. – 2012. – **2**. – P. 471–479.
40. *Wang Y., Panzik J. E., Kiefer B., Lee K. K. M.* Crystal structure of graphite under room-temperature compression and decompression // Ibid. – 2012. – **2**. – P. 520–527.
41. *Xu J.-A., Mao H.-K., Hemley R. J.* The gem anvil cell: high-pressure behaviour of diamond and related materials // J. Phys. Condens. Matter. – 2002. – **14**. – P. 11549–11552.
42. *Boulfelfel S. E., Seifert G., Grin Yu., Leoni S.* Squeezing lone pairs: the A17 to A7 pressure-induced phase transition in black phosphorus // Phys. Rev. B. – 2012. – **85**, art. 014110.
43. *Zahn D., Leoni S.* Nucleation and growth in pressure-induced phase transitions from molecular dynamics simulations: mechanism of the reconstructive transformation of NaCl to the CsCl-type structure // Phys. Rev. Lett. – 2004. – **92**, art. 250201.
44. *Boulfelfel S. E., Leoni S.* Competing intermediates in the pressure-induced wurtzite to rock-salt phase transition in ZnO // Phys. Rev. B. – 2008. – **78**, art. 125204.
45. *Leoni S., Zahn D.* Putting the squeeze on NaCl: modeling and simulation of the pressure driven B1–B2 phase transition // Z. Kristallogr. – 2004. – **219**. – P. 339–344.
46. *Boulfelfel S. E., Zahn D., Grin Yu., Leoni S.* Walking the path from B4- to B1-type structures in GaN // Phys. Rev. Lett. – 2007. – **99**, art. 125505.

Stony Brook University
Moscow State University

Received 21.09.2012